

# Synergistic effect of a combination of nanoparticulate $\text{Fe}_3\text{O}_4$ and gambogic acid on phosphatidylinositol 3-kinase/Akt/Bad pathway of LOVO cells

Lianghua Fang<sup>1,3</sup>  
Baoran Chen<sup>2</sup>  
Shenlin Liu<sup>3</sup>  
Ruiping Wang<sup>3</sup>  
Shouyou Hu<sup>3</sup>  
Guohua Xia<sup>2</sup>  
Yongli Tian<sup>3</sup>  
Xiaohui Cai<sup>2</sup>

<sup>1</sup>No 1 Clinical Medical College of Nanjing University of Chinese Medicine, <sup>2</sup>Department of Hematology, Zhongda Hospital, Medical School, Southeast University, <sup>3</sup>Department of Oncology, Jiangsu Province Hospital of Traditional Chinese Medicine, Nanjing, People's Republic of China

**Background:** The present study evaluated whether magnetic nanoparticles containing  $\text{Fe}_3\text{O}_4$  could enhance the activity of gambogic acid in human colon cancer cells, and explored the potential mechanisms involved.

**Methods:** Cytotoxicity was evaluated by MTT assay. The percentage of cells undergoing apoptosis was analyzed by flow cytometry, and cell morphology was observed under both an optical microscope and a fluorescence microscope. Reverse transcriptase polymerase chain reaction and Western blot assay were performed to determine the transcription of genes and expression of proteins, respectively.

**Results:** Gambogic acid could inhibit proliferation of LOVO cells in a dose-dependent and time-dependent manner and induce apoptosis, which was dramatically enhanced by magnetic nanoparticles containing  $\text{Fe}_3\text{O}_4$ . The typical morphological features of apoptosis in LOVO cells were observed after treatment comprising gambogic acid with and without magnetic nanoparticles containing  $\text{Fe}_3\text{O}_4$ . Transcription of cytochrome c, caspase 9, and caspase 3 genes was higher in the group treated with magnetic nanoparticles containing  $\text{Fe}_3\text{O}_4$  and gambogic acid than in the groups that received gambogic acid or magnetic nanoparticles containing  $\text{Fe}_3\text{O}_4$ , but transcription of phosphatidylinositol 3-kinase, Akt, and Bad genes decreased. Notably, expression of cytochrome c, caspase 9, and caspase 3 proteins in the group treated with gambogic acid and magnetic nanoparticles containing  $\text{Fe}_3\text{O}_4$  was higher than in the groups receiving magnetic nanoparticles containing  $\text{Fe}_3\text{O}_4$  or gambogic acid, while expression of p-PI3K, p-Akt, p-Bad, pro-caspase 9, and pro-caspase 3 degraded.

**Conclusion:** Magnetic nanoparticles containing  $\text{Fe}_3\text{O}_4$  can enhance apoptosis induced by gambogic acid which may be closely related to regulation of the PI3K/Akt/Bad pathway in the treatment of human colon cancer.

**Keywords:**  $\text{Fe}_3\text{O}_4$ , magnetic nanoparticles, gambogic acid, LOVO cells, apoptosis, PI3K, Akt, Bad, pathway

## Introduction

Despite the availability of chemical and molecular targeted drugs, almost 80% of patients with colorectal cancer in China rely on traditional Chinese medicine therapy. A number of studies have been performed recently to assess the therapeutic efficacy and safety of traditional Chinese medicine for treating cancer.<sup>1,2</sup> It is noteworthy that gambogic acid, a major ingredient isolated from the Chinese herb *Gamboge hanburyi*, can not only inhibit cell growth, induce apoptosis, and arrest the cell cycle in various

Correspondence: Ruiping Wang  
Department of Oncology, Jiangsu  
Province Hospital of Traditional  
Chinese Medicine, Nanjing 210029,  
People's Republic of China  
Tel +86 138 1588 3181  
Fax +86 025 8661 7141  
Email wrp61@163.com

carcinoma cell lines, including pulmonary carcinoma,<sup>3</sup> hepatocellular carcinoma,<sup>4</sup> breast cancer,<sup>5</sup> prostate cancer,<sup>6</sup> and gastric cancer,<sup>7</sup> but it can also inhibit tumor cell proliferation and inhibit angiogenesis by suppressing the phosphorylation of Akt, Erk, c-Src, Fak, and vascular endothelial growth factor receptor 2.<sup>8,9</sup> These findings suggest that gambogic acid may indeed be an effective agent in the treatment of cancer. However, to date, the potential mechanisms that account for the beneficial effects of gambogic acid remain largely unknown.

Recently, magnetic nanoparticles containing  $\text{Fe}_3\text{O}_4$ , which have excellent biocompatibility<sup>10</sup> and improved intracellular penetration,<sup>11,12</sup> have become a focus for potential application in human medicine, including the delivery of anticancer drugs to overcome drug resistance and enhance the effectiveness of chemotherapy.<sup>12,13</sup> Accumulating research has shown that not only can a combination of magnetic nanoparticles containing  $\text{Fe}_3\text{O}_4$  and adriamycin have a significant cytotoxic effect on drug-resistant K562/A02 leukemia cells,<sup>14,15</sup> but also that a combination of magnetic nanoparticles containing  $\text{Fe}_3\text{O}_4$  and antitumor drugs may interact synergistically to induce apoptosis in cancer cells. Further, it has been shown that the cytotoxicity and apoptosis induced by gambogic acid in cancer cells can be dramatically enhanced if gambogic acid is combined with magnetic nanoparticles containing  $\text{Fe}_3\text{O}_4$ ,<sup>16</sup> but the signal transduction pathways accounting for the beneficial effects of gambogic acid remain largely unknown.

It is well known that apoptosis is a major mechanism of cell death. The phosphatidylinositol 3-kinase (PI3K/Akt) pathway acts as a critical regulator of cell survival by stimulating cell proliferation and inhibiting apoptosis, and abnormal signal transduction pathways are important in tumorigenesis and tumor progression.<sup>17</sup> Bad, a member of the Bcl-2 family, is one of several substrates for Akt.<sup>18</sup> Phosphorylation of Bad by Akt suppresses its auxo-apoptotic functions, accounting in part for the potent survival function of Akt.<sup>18</sup> Close attention has been paid to identify new target drugs that block signal transduction pathways in cancer cells.<sup>19</sup> Overexpression of PI3K/Akt pathway components, such as PI3K/p85 $\alpha$ , Akt1, and Akt2, may contribute to the growth and progression of colorectal cancer.<sup>20,21</sup> Therefore, it may be that a strategy of targeted inhibition in PI3K/Akt pathway components could increase sensitivity to chemotherapy and decrease the metastatic capacity of colorectal cancer cells.<sup>19,22–24</sup> At present, there are many compounds that target PI3K (or Akt) progressing through clinical trials. However, to the best of our knowledge, there has been no

study of the effect of magnetic nanoparticles containing a combination of gambogic acid and  $\text{Fe}_3\text{O}_4$  in the PI3K/Akt/Bad pathway in colon cancer cells. Given the role of the PI3K/Akt signaling pathway, our aim in these experiments was to investigate the effect of magnetic nanoparticles containing  $\text{Fe}_3\text{O}_4$  and gambogic acid on LOVO cells and the potential role of this signaling pathway in the treatment of human colon cancer.

## Materials and methods

### Main materials

Gambogic acid (Kanion Pharmaceutical Co, Ltd, Jiangsu, China) was dissolved in dimethyl sulfoxide (Sigma-Aldrich, St Louis, MO), stored at  $-20^\circ\text{C}$ , and then diluted as needed in RPMI 1640 medium (Gibco/BRL, Carlsbad, CA). Methylthiazol tetrazolium (MTT) and propidium iodide were purchased from Sigma-Aldrich (St Louis, CA).  $\text{Fe}_3\text{O}_4$  magnetic nanoparticles (State Key Laboratory of Bioelectronics, Nanjing, China) were well distributed in RPMI 1640 medium containing 10% (v/v) heat-inactivated new-born calf serum (Sijiqing, Hangzhou, China) using an ultrasonic generator (Kudos SK3300HP, 53 kHz, maximum power 180 W, Kudos Ultrasonic Instrument Limited, Shanghai, China) to obtain a colloidal suspension of  $\text{Fe}_3\text{O}_4$  magnetic nanoparticles. Gambogic acid was conjugated with the magnetic nanoparticles containing  $\text{Fe}_3\text{O}_4$  by mechanical absorption polymerization at  $4^\circ\text{C}$  for 48 hours,<sup>16</sup> and their size was approximately 50 nm. 4, 6-diamidino-2-phenylindole (DAPI) was obtained from Santa Cruz Biotechnology Inc (Santa Cruz, CA). An Annexin V-fluorescein isothiocyanate kit was obtained from Nanjing Keygen Biotech Co, Ltd (Nanjing, China), and Trizol reagent was from Invitrogen Life Technologies (Carlsbad, CA). Monoclonal antibodies of PI3K, p-PI3K, Akt, p-Akt, Bad, p-Bad, cytochrome c, caspase 9, caspase 3, and  $\beta$ -actin were from Santa Cruz Biotechnology Inc.

### Cell culture

A human colorectal cancer cell line (LOVO) purchased from Nanjing Keygen Biotech Co, Ltd was cultured in RPMI 1640 medium containing 10% (v/v) heat-inactivated new-born calf serum, penicillin G 100 U/mL, and streptomycin 100  $\mu\text{g}$ /mL at  $37^\circ\text{C}$  in a humidified environment containing 5%  $\text{CO}_2$ .

### Cell proliferation assay

Cytotoxicity was determined by MTT assay. Exponentially growing LOVO cells were seeded in 96-well plates (Costar, Fisher Scientific, Hampton, NH) in RPMI 1640 medium containing 10% new-born calf serum at a density of

$5 \times 10^3$  cells/well for 24 hours. Based on our previous studies<sup>16</sup> of the characteristics of magnetic nanoparticles containing Fe<sub>3</sub>O<sub>4</sub>, the cells were treated with different concentrations of magnetic nanoparticles containing Fe<sub>3</sub>O<sub>4</sub> and/or gambogic acid for 12, 24, and 48 hours. Meanwhile, RPMI 1640 medium was used as the blank control. Then, 20  $\mu$ L of MTT 0.5 mg/mL were added to each well and cultured for another 4 hours. Thereafter, the formazan was dissolved with 150  $\mu$ L of dimethyl sulfoxide after blotting the culture medium. Finally, the plates were shaken lightly for 10 minutes and the reduction of MTT was quantified by absorbance at a wave length of 540 nm using a microplate reader (Model-550, Bio-Rad Laboratories, Hercules, CA). The cell inhibition ratio (%) was calculated as  $(1 - A_{\text{treated group}}/A_{\text{control group}}) \times 100$ . Each assay was repeated at least three times.

### Apoptosis assay by flow cytometry

Based on the results of the cytotoxicity assay, the minimum inhibition concentration of gambogic acid and its combination with magnetic nanoparticles containing Fe<sub>3</sub>O<sub>4</sub> was used to measure the apoptosis rate in LOVO cells by flow cytometry. Briefly, after treatment with gambogic acid 0.35  $\mu$ mol/L, 60  $\mu$ g/mL Fe<sub>3</sub>O<sub>4</sub> magnetic nanoparticles, or nanoparticles containing gambogic acid and Fe<sub>3</sub>O<sub>4</sub> (0.35  $\mu$ mol/L gambogic acid with 60  $\mu$ g/mL Fe<sub>3</sub>O<sub>4</sub> magnetic nanoparticles) for 48 hours. LOVO cells were collected, washed twice with ice-cold phosphate-buffered solution, and then suspended in 200  $\mu$ L of binding buffer and 10  $\mu$ L of Annexin V-fluorescein isothiocyanate for 15 minutes in the dark. Thereafter, 300  $\mu$ L of binding buffer and 5  $\mu$ L of propidium iodide were added to each sample. Finally, the cells were analyzed using BD FACS Diva flow cytometry (BD FACS Canto TM II) with FACSCalibur CellQuest™

software, and the results are expressed as the mean of three individual experiments.

### Assessment of cell morphology

For assessment of cell morphology, LOVO cells were incubated for 48 hours as described earlier. The cells were then collected and stained with Wright's stain to observe the morphological changes in cells undergoing apoptosis by optical microscopy. Meanwhile, cells on other slides were fixed with methanol for 15 minutes, stained with DAPI fluorochrome dye, and then observed under a fluorescence microscope ( $1 \times 51$ ; Olympus, Tokyo, Japan) with a peak excitation wave length of 340 nm.

### Reverse transcriptase PCR assay

As described for the apoptosis assay, the treated LOVO cells were harvested and their total RNA content was then isolated using Trizol reagent according to the manufacturer's protocol. The reverse transcription reactions were performed using SuperScript™ II reverse transcriptase, and the newly synthetic cDNA was amplified within target and control sequences (Table 1). Polymerase chain reaction (PCR) products were separated on 1% agarose gel and visualized with ethidium bromide staining using a Molecular Imager Gel Doc XR system (Bio-Rad, CA, USA), and quantified using Molecular Analyst software version 1.5 (Bio-Rad), with  $\beta$ -actin as an internal control for all genes. The relative value was calculated as the ratio of each group and the internal control group. The results are expressed as the mean value of three individual experiments.

### Western blot assay

Western blot analysis was performed to examine the expression of PI3K, p-PI3K, Akt, p-Akt, Bad, p-Bad, cytochrome c,

**Table 1** Sequences of gene-specific primers

Gene	Primer	Band size (bp)	Annealing temperature (°C)
$\beta$ -actin	Forward 5'-GTCACCAACTGGGACGACATG-3' Reverse 5'-GCCGTCAGGCAGCTCGTAGC-3'	510	55
PI3K	Forward 5'-CTGTGTGGGACTTATTGAGGTGGTGC-3' Reverse 5'-GGCATGCTGTCTGAATAGCTAGATAAGC-3'	457	52
Akt	Forward 5'-ATGAGCGACGTGGCTATTGTGAAG-3' Reverse 5'-GAGGCCGTCAGCCACAGTCTGGATG-3'	330	52
Bad	Forward 5'-GCTCTTCCTTT GTTCATCTCC-3' Reverse 5'-CATCTGGCTCGGGGTTACTGC-3'	304	50
Cytochrome c	Forward 5'-CGCCAATAAGAACAAGG-3' Reverse 5'-AATCAGGACTGCCCAACA-3'	304	50
Caspase 9	Forward 5'-GCTCTTCCTTTGTTCATCTCC-3' Reverse 5'-CATCTGGCTCGGGGTTACTGC-3'	742	52
Caspase 3	Forward 5'-TTCAGAGGGGATCGTTGTAGAAGTC-3' Reverse 5'-5-CAAGCTTGTCGGCATACTGTTTCAG-3'	264	57

pro-caspase 9, caspase 9, pro-caspase 3, and caspase 3. In brief, total protein was isolated on ice and subjected to 10% sodium dodecyl sulfate polyacrylamide gel electrophoresis using modified radioimmunoprecipitation assay buffer, and then transferred to a polyvinylidene difluoride membrane (65421, Pall Corporation, Port Washington, NY). The membrane was blocked with buffer containing 10% fat-free dry milk and performed with 1:200 dilution of monoclonal antibodies against either antihuman PI3K, p-PI3K, Akt, p-Akt, Bad, p-Bad, cytochrome c, pro-caspase 9, caspase 9, pro-caspase 3, caspase 3, or  $\beta$ -actin antibody, and then subsequently incubated with horseradish peroxidase-conjugated goat antirabbit (1:5000) as a secondary antibody. The band was detected using an enhanced chemiluminescence detection system (Amersham, Buckinghamshire, UK). Each value is presented as the relative density of protein bands normalized to  $\beta$ -actin.

## Statistical analysis

All data are expressed as the mean  $\pm$  standard deviation from triplicate experiments and analyzed using the statistical Package for Social Science (SPSS Release 13.0, IBM, Chicago, IL). The statistical significance of differences was determined by the Student's *t*-test in two groups and one-way analysis of variance among multiple groups. A *P* value  $< 0.05$  was considered to be statistically significant.

## Results

### Inhibition of cell growth

Inhibition of LOVO cell growth was markedly lower when the concentration of gambogic acid was less than 0.35  $\mu\text{mol/L}$  (Figure 1A); however, the inhibition rate was increased in a dose-dependent and time-dependent manner when the dosage of gambogic acid was more than 0.35  $\mu\text{mol/L}$ , suggesting that the minimum inhibition rate of gambogic acid was 0.35  $\mu\text{mol/L}$ . Further, it was observed that addition of magnetic nanoparticles containing  $\text{Fe}_3\text{O}_4$  enhanced the inhibition of LOVO cells by gambogic acid, and 50% inhibition achieved by gambogic acid was reduced from 0.60  $\mu\text{mol/L}$  to 0.41  $\mu\text{mol/L}$  by 60  $\mu\text{g/mL}$  magnetic nanoparticles containing a combination of  $\text{Fe}_3\text{O}_4$  and gambogic acid ( $P < 0.05$ , Figure 1B), suggesting that this combination had a synergistic effect on apoptosis of LOVO cells.

### Synergistic effect on apoptosis of LOVO cells

The data show that the proportion of apoptotic cells was higher in the gambogic acid group than that in the control

group (20.12%  $\pm$  2.32% versus 9.04%  $\pm$  2.16%,  $P < 0.05$ ), but there was no significant difference between the group treated with magnetic nanoparticles containing  $\text{Fe}_3\text{O}_4$  and the control group (8.21%  $\pm$  1.67% versus 9.04%  $\pm$  2.16%,  $P > 0.05$ ). Most notably, the apoptosis ratio was significantly increased (50.63%  $\pm$  4.95%) when 0.35  $\mu\text{mol/L}$  gambogic acid was combined with 60  $\mu\text{g/mL}$  magnetic nanoparticles containing  $\text{Fe}_3\text{O}_4$ , indicating that magnetic nanoparticles containing  $\text{Fe}_3\text{O}_4$  could enhance the apoptosis induced by gambogic acid (Figure 2).

### Morphological changes in LOVO cells

LOVO cells in the control group and in the group treated with magnetic nanoparticles containing  $\text{Fe}_3\text{O}_4$  had a normal healthy shape, as demonstrated by their clear cytoskeletons (Figure 3A and B). After treatment consisting of 60  $\mu\text{g/mL}$  magnetic nanoparticles containing  $\text{Fe}_3\text{O}_4$  with or without 0.35  $\mu\text{mol/L}$  gambogic acid for 48 hours, typical cytomorphological features of apoptosis in LOVO cells were observed, ie, cell shrinkage, chromatin condensation, margination, and presence of apoptotic bodies (Figure 3C and D). Moreover, under the fluorescence microscope, LOVO cells in the control group and in the  $\text{Fe}_3\text{O}_4$  magnetic nanoparticle group stained equally with blue fluorescence, indicating that chromatin was distributed in the nucleolus to a similar extent (Figure 4A and B), but that 0.35  $\mu\text{mol/L}$  gambogic acid induced a proportion of LOVO cells to display chromatin condensation and pyknosis of the nucleolus (Figure 4C). After incubation with magnetic nanoparticles containing  $\text{Fe}_3\text{O}_4$  and gambogic acid (0.35  $\mu\text{mol/L}$  gambogic acid with 60  $\mu\text{g/mL}$   $\text{Fe}_3\text{O}_4$  magnetic nanoparticles) for 48 hours, the proportion of cells emitting bright fluorescence increased and showed the typical features of apoptosis, including chromatin condensation, pyknosis of the nucleolus, and nuclear fragmentation (Figure 4D).

### Transcription of apoptosis-related genes by reverse transcriptase PCR

Transcription of apoptosis-related genes was not influenced by 60  $\mu\text{g/mL}$   $\text{Fe}_3\text{O}_4$  magnetic nanoparticles, but nanoparticles containing  $\text{Fe}_3\text{O}_4$  and gambogic acid (0.35  $\mu\text{mol/L}$  gambogic acid with 60  $\mu\text{g/mL}$   $\text{Fe}_3\text{O}_4$  magnetic nanoparticles) could dramatically upregulate the transcription of cytochrome c, caspase 9, and caspase 3 genes in LOVO cells when compared with the control group ( $P < 0.05$ ), surpassing the effects of 0.35  $\mu\text{mol/L}$  gambogic acid alone (Figure 5,  $P < 0.05$ ), while downregulating transcription of PI3K, Akt, and Bad genes in LOVO cells when compared with

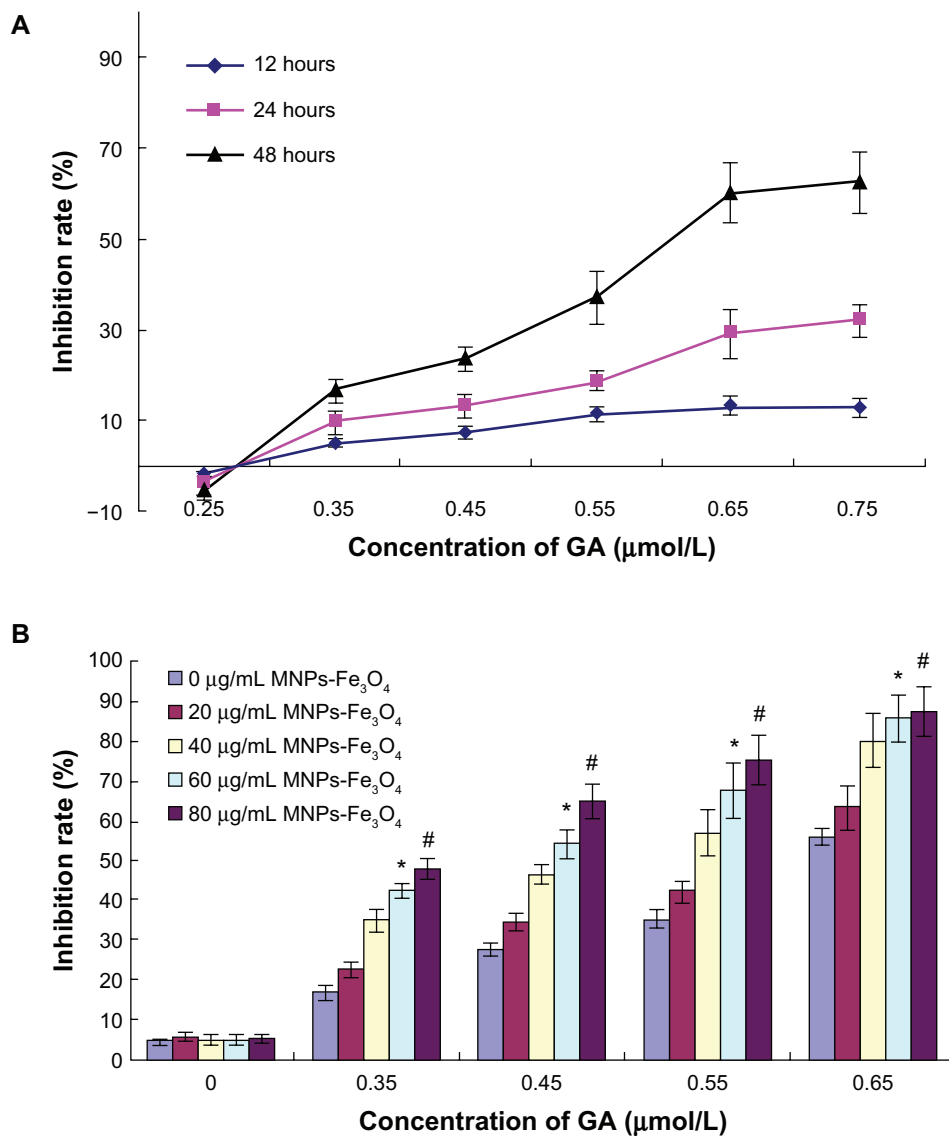


**Figure 1** (A) Inhibition rate of LOVO cells treated with various concentrations of GA for different times. (B) Inhibition rate of LOVO cells treated with the combination of GA and Fe<sub>3</sub>O<sub>4</sub> magnetic nanoparticles for 48 hours.

**Notes:** \* $P < 0.05$  when compared with controls; # $P > 0.05$  when compared with the group treated with Fe<sub>3</sub>O<sub>4</sub> magnetic nanoparticles.

**Abbreviations:** MNPs-Fe<sub>3</sub>O<sub>4</sub>, magnetic nanoparticles of Fe<sub>3</sub>O<sub>4</sub>; GA, gambogic acid.

the control group ( $P < 0.05$ ), also surpassing the effects of 0.35 μmol/L gambogic acid alone ( $P < 0.05$ , Figure 5).

## Expression of apoptosis-related proteins by Western blot assay

Based on computer-assisted image analysis, it seems that apoptosis-related proteins in LOVO cells treated with 60 μg/mL Fe<sub>3</sub>O<sub>4</sub> magnetic nanoparticles showed no significant changes when compared with the control group ( $P > 0.05$ ). However, cytochrome c, caspase 3, and caspase 9 protein levels in LOVO cells treated with 0.35 μmol/L gambogic acid increased dramatically when compared with the control group ( $P < 0.05$ , Figure 6), and upregulation

was enhanced by the magnetic nanoparticles containing Fe<sub>3</sub>O<sub>4</sub> ( $P < 0.05$ ). Conversely, compared with the control group, p-PI3K, p-Akt, p-Bad, pro-caspase 9, and pro-caspase 3 protein expression in LOVO cells treated with magnetic nanoparticles containing Fe<sub>3</sub>O<sub>4</sub> and gambogic acid was lower than that in cells treated with 0.35 μmol/L gambogic acid alone ( $P < 0.05$ , Figure 6), but there were no significant differences in levels of nonactivated proteins, including PI3K, Akt, and Bad in these four groups ( $P > 0.05$ , Figure 6).

## Discussion

The ultimate goal of medical cancer research is to be able to manipulate the machinery of cell death. Regulation of

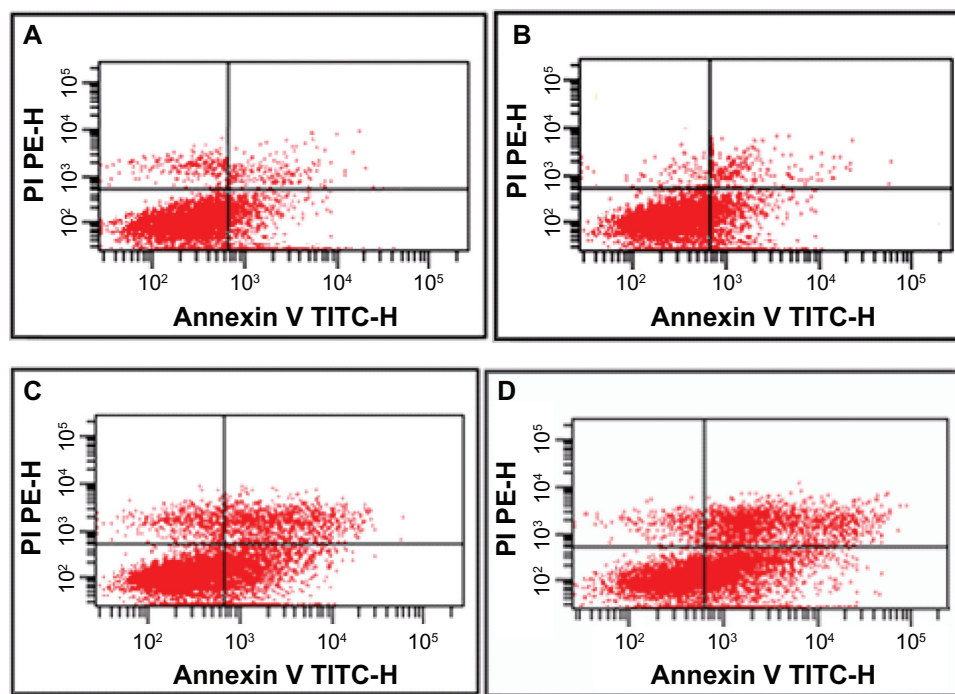


**Figure 2** Apoptosis ratio of LOVO cells treated with gambogic acid,  $\text{Fe}_3\text{O}_4$  magnetic nanoparticles, or magnetic nanoparticles containing  $\text{Fe}_3\text{O}_4$  and gambogic acid for 48 hours. (A) Controls, (B) 60  $\mu\text{g}/\text{mL}$  magnetic nanoparticles containing  $\text{Fe}_3\text{O}_4$ , (C) 0.35  $\mu\text{mol}/\text{L}$  gambogic acid, and (D) magnetic nanoparticles containing  $\text{Fe}_3\text{O}_4$  and gambogic acid (0.35  $\mu\text{mol}/\text{L}$  gambogic acid and 60  $\mu\text{g}/\text{mL}$  magnetic nanoparticles containing  $\text{Fe}_3\text{O}_4$ ).

apoptosis could lead to new possibilities for cancer therapy. Previous studies<sup>25,26</sup> have shown that gambogic acid can induce apoptosis via alteration of different molecules associated with apoptosis, such as Bax/Bcl-2 and nuclear factor- $\kappa\text{B}$ . Recently, the synergistic effects of magnetic nanoparticles containing  $\text{Fe}_3\text{O}_4$  and gambogic acid in the apoptosis of

leukemia cells were demonstrated.<sup>16</sup> Accumulating research findings have shown that nanotechnology and nanoparticles are becoming a focus for application in clinical medicine because of their stable biomolecular absorption, high surface energy, and small size comparable with biomolecules.<sup>27,28</sup> Our present study shows that gambogic acid can inhibit

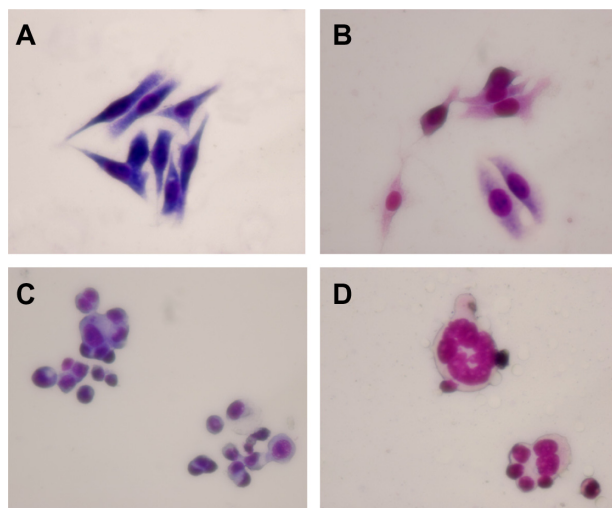


**Figure 3** Morphological features of LOVO cells after treatment for 48 hours by optical microscope ( $\times 400$ , Wright staining). (A) Controls, (B) 60  $\mu\text{g}/\text{mL}$  magnetic nanoparticles containing  $\text{Fe}_3\text{O}_4$ , (C) 0.35  $\mu\text{mol}/\text{L}$  gambogic acid, and (D) magnetic nanoparticles containing  $\text{Fe}_3\text{O}_4$  and gambogic acid (0.35  $\mu\text{mol}/\text{L}$  gambogic acid with 60  $\mu\text{g}/\text{mL}$  magnetic nanoparticles containing  $\text{Fe}_3\text{O}_4$ ).

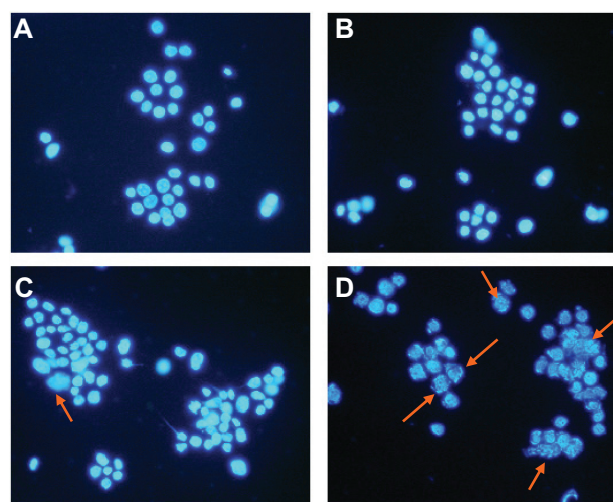


**Figure 4** Nucleolus morphological changes of LOVO cells after treatment for 48 hours under fluorescence microscope ( $\times 400$ , DAPI staining). (A) Controls, (B) 60  $\mu\text{g}/\text{mL}$  magnetic nanoparticles containing  $\text{Fe}_3\text{O}_4$ , (C) 0.35  $\mu\text{mol}/\text{L}$  gambogic acid, and (D) magnetic nanoparticles containing  $\text{Fe}_3\text{O}_4$  and gambogic acid (0.35  $\mu\text{mol}/\text{L}$  gambogic acid with 60  $\mu\text{g}/\text{mL}$  magnetic nanoparticles containing  $\text{Fe}_3\text{O}_4$ ).

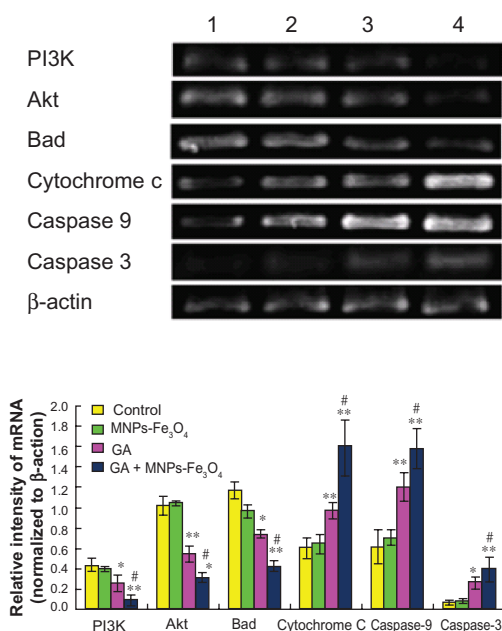


**Figure 5** Transcription of PI3K, Akt, Bad, cytochrome C, caspase 9, and caspase 3 gene in LOVO cells after treatment comprising GA with or without MNPs-Fe<sub>3</sub>O<sub>4</sub> for 48 hours.

**Notes:** Lane 1, controls; Lane 2, 60 µg/mL MNPs-Fe<sub>3</sub>O<sub>4</sub>; Lane 3, 0.35 µmol/L GA; Lane 4, GA-MNPs-Fe<sub>3</sub>O<sub>4</sub> (0.35 µmol/L GA with 60 µg/mL MNPs-Fe<sub>3</sub>O<sub>4</sub>). \**P* < 0.05; \*\**P* < 0.01, when compared with control group; #*P* < 0.05, when compared with the GA group.

**Abbreviations:** MNPs-Fe<sub>3</sub>O<sub>4</sub>, magnetic nanoparticles containing Fe<sub>3</sub>O<sub>4</sub>; GA, gambogic acid.

proliferation of LOVO cells in a dose-dependent and time-dependent manner, and that this is enhanced by magnetic nanoparticles containing Fe<sub>3</sub>O<sub>4</sub>. In particular, there was no significant inhibition of LOVO cells when the concentration of magnetic nanoparticles containing Fe<sub>3</sub>O<sub>4</sub> was in the range of 20–80 µg/mL (Figure 1B), indicating that magnetic nanoparticles containing Fe<sub>3</sub>O<sub>4</sub> themselves had no cytotoxicity, which is consistent with current research.<sup>29</sup> Our study also provides evidence that the apoptosis ratio in LOVO cells treated with an optimal combination of gambogic acid and Fe<sub>3</sub>O<sub>4</sub> magnetic nanoparticles increased dramatically compared with cells treated with gambogic acid alone (*P* < 0.05, Figure 2), which confirms that magnetic nanoparticles containing Fe<sub>3</sub>O<sub>4</sub> and gambogic acid have a synergistic effect on LOVO cells. At the same time, under optical microscopy (Figure 3) and fluorescence microscopy (Figure 4), typical features of apoptosis, including chromatin condensation, pyknosis of the nucleolus, and apoptotic bodies, were observed when LOVO cells were treated using gambogic acid with or without magnetic nanoparticles containing Fe<sub>3</sub>O<sub>4</sub> for 48 hours. Of note, the proportion of apoptotic cells in the gambogic acid group was less than that in the group receiving magnetic nanoparticles containing Fe<sub>3</sub>O<sub>4</sub> and gambogic acid.

However, no cell morphology typical of apoptosis was seen in either the group receiving magnetic nanoparticles containing Fe<sub>3</sub>O<sub>4</sub> or in the control group, and this result was confirmed by flow cytometry (Figure 2).

In order to explore the potential mechanisms of action of gambogic acid, we investigated the status of the PI3K/Akt signaling pathway, components of which are often overexpressed in colorectal cancer and play important roles in the growth and progression of the disease.<sup>20,21</sup> An earlier study demonstrated that 2-(4-morpholinyl)-8-phenyl-1(4H)-benzopyran-4-one hydrochloride and wortmannin, both known PI3K inhibitors, showed antitumorigenic activity in human colon cancer cells in vivo and could cause induction of apoptosis and cell growth arrest in several colorectal cancer cell lines.<sup>30,31</sup> Our present data show that treatment with gambogic acid markedly inhibited the activity of PI3K at the transcriptional and translation levels, and that the mRNA of PI3K and the protein of the activated form of PI3K were substantially reduced (Figures 5 and 6). These variations were more significant when combined with magnetic nanoparticles containing Fe<sub>3</sub>O<sub>4</sub>. Nevertheless, differences between the Fe<sub>3</sub>O<sub>4</sub> magnetic nanoparticle and control groups were not found. It is well known that protein translation follows gene transcription, but mRNA and protein were detected simultaneously in our study, and this may explain why no obvious changes were found in total PI3K protein, although the mRNA and activated protein for PI3K were changed. This phenomenon was also found in later indices, including expression of Akt and Bad proteins.

As previously reported, Akt is the best known downstream target of PI3K, which binds PIP<sub>3</sub> at the plasma membrane, and this leads to phosphorylation of Akt at Ser-473 in its regulatory domain.<sup>32</sup> It has also been reported that inactivation of PI3K inhibits phosphorylation of Akt.<sup>33</sup> Consistent with prior research, our study revealed that downregulation of Akt mRNA and the p-Akt (Ser-473) protein was accompanied by inactivation of PI3K in LOVO cells treated with gambogic acid alone. Furthermore, inhibition of Akt was markedly enhanced when combined with magnetic nanoparticles containing Fe<sub>3</sub>O<sub>4</sub> (*P* < 0.05, Figures 5 and 6). Liu et al<sup>34</sup> reported recently that Akt, as a hinge in the signal transduction pathway, can regulate cell proliferation, apoptosis, and the cell cycle via a number of downstream molecules. It is worthwhile noting that it could directly or indirectly regulate apoptosis through the mitochondrial pathway. Bad is the first member of the Bcl-2 family found to be a substrate of Akt, and nonphosphorylated Bad is an activated state. It could be phosphorylated at Ser-136 by activation and phosphorylation

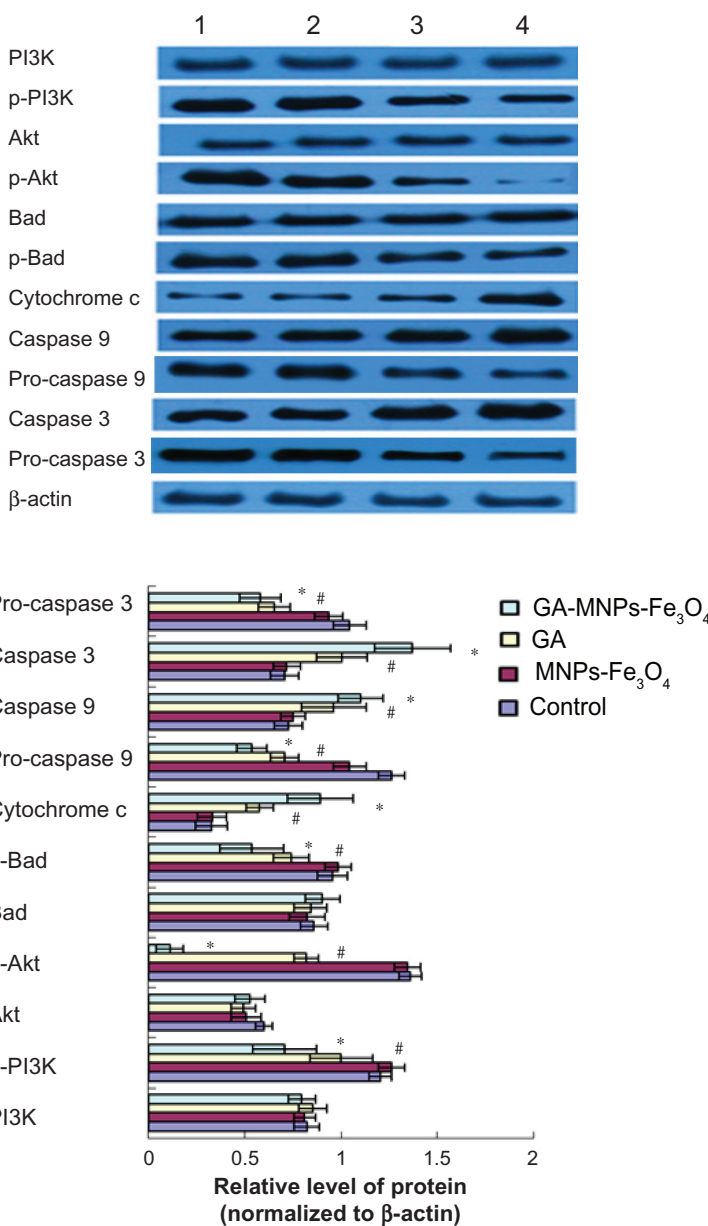


**Figure 6** Expression of PI3K, p-PI3K, Akt, p-Akt, Bad, p-Bad, cytochrome c, pro-caspase 9, caspase 9, and pro-caspase 3, caspase 3 proteins in LOVO cells after treatment comprising GA with or without MNPs-Fe<sub>3</sub>O<sub>4</sub> for 48 hours.

**Notes:** Lane 1, control; lane 2, 60 μg/mL MNPs-Fe<sub>3</sub>O<sub>4</sub>; lane 3, 0.35 μmol/L GA; lane 4, GA-MNPs-Fe<sub>3</sub>O<sub>4</sub> (0.35 μmol/L GA with 60 μg/mL MNPs-Fe<sub>3</sub>O<sub>4</sub>). \**P* < 0.05, \*\**P* < 0.01 compared with the control group; #*P* < 0.05, when compared with the GA group.

**Abbreviations:** MNPs-Fe<sub>3</sub>O<sub>4</sub>, magnetic nanoparticles containing Fe<sub>3</sub>O<sub>4</sub>; GA, gambogic acid.

of Akt,<sup>35</sup> then separated from the heterodimer of Bcl-2/Bcl-xL, bound to 14-3-3 scaffold proteins, and localized in the cytoplasm in an inactive form, thus playing an antiapoptotic effect.<sup>36</sup> Kim et al showed that phosphorylated Bad was increased in colorectal cancer cells, which may alter regulation of cell death during colorectal tumorigenesis.<sup>37</sup> Therefore, inhibition of Bad phosphorylation could be a promising way of treating or preventing colorectal cancer. To elucidate whether apoptosis induced by gambogic acid was

through the mitochondrial pathway associated with the PI3K/Akt/Bad signal transduction pathway, we then explored the status of Bad and its downstream molecules in LOVO cells. Our present study demonstrated that gambogic acid markedly reduced Bad mRNA and inhibited phosphorylation of Bad, especially its protein (Figure 6). Moreover, the literature reports that overexpression of phospho-Akt correlates with phosphorylation of epithelial growth factor receptor, FKHR, and Bad in nasopharyngeal carcinoma.<sup>38</sup> Thus, we infer that



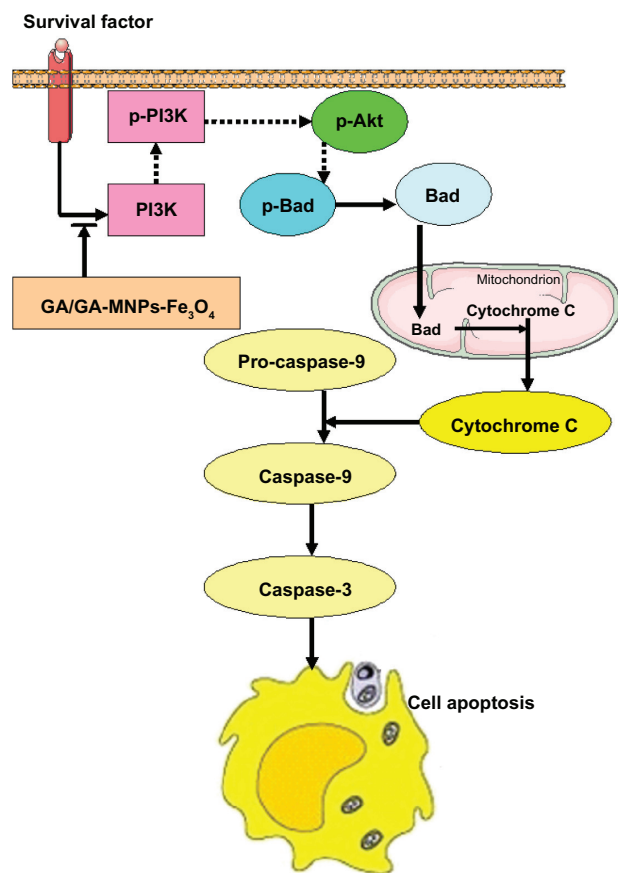


**Figure 7** The mechanism of GA/GA-MNPs-Fe<sub>3</sub>O<sub>4</sub> on apoptosis of LOVO cells.

**Notes:** →, Promote; ---, inhibit; ⊣, block.

**Abbreviations:** MNPs-Fe<sub>3</sub>O<sub>4</sub>, magnetic nanoparticles containing Fe<sub>3</sub>O<sub>4</sub>; GA, gambogic acid.

these variations would be the result of the Akt signal being abrogated by gambogic acid. The crucial step in induction of apoptosis of dephosphorylated Bad requires release of cytochrome c into the cytoplasm, which provokes an apoptotic cascade.<sup>39</sup> In our study, it was found that levels of cytochrome c, mRNA, and protein were notably increased along with the decrease of phosphorylated Bad. Most notably, these variations in the group treated with magnetic nanoparticles containing Fe<sub>3</sub>O<sub>4</sub> and gambogic acid were more conspicuous than those in the group treated with gambogic acid alone. It has been shown that cytochrome c catalyzes oligomerization of apoptotic protease activating factor-1, which recruits and promotes activation of pro-caspase 9.<sup>39</sup> This, in turn, cleaves and activates the effector caspase 3, leading to apoptosis.<sup>39</sup> Our data show that, when accompanied by activation of cytochrome c, the activator caspase 9 and the executor caspase 3 are also activated, along with upregulation of the mRNAs for caspase 9 and caspase 3, and the proteins of cleaved caspase 9 and cleaved caspase 3 are detected. It is noteworthy that levels of mRNA and proteins for caspase 9

and caspase 3 in the group treated with a combination of magnetic nanoparticles containing Fe<sub>3</sub>O<sub>4</sub> and gambogic acid were higher than those in the group treated with gambogic acid alone, which confirms further that gambogic acid and magnetic nanoparticles containing Fe<sub>3</sub>O<sub>4</sub> have a synergistic effect on LOVO cells.

In light of the present data and previous findings, we believe that gambogic acid can stop PI3K transmitting a mitogenic signal to Akt, followed by activation of Bad, leading to release of cytochrome c and activation of caspase 9 and caspase 3. These events may be responsible for the apoptosis shown in Figure 7. Notably, these effects are potentiated by the combination of Fe<sub>3</sub>O<sub>4</sub> magnetic nanoparticles and gambogic acid.

## Conclusion

Our study demonstrates for the first time that the combination of Fe<sub>3</sub>O<sub>4</sub> magnetic nanoparticles and gambogic acid has a synergistic effect on the inhibition and apoptosis of LOVO cells, which may be closely associated with regulation of the PI3K/Akt/Bad pathway. This provides theoretical evidence of a clinical benefit for patients with colorectal cancer, and further research is planned in the future.

## Acknowledgments

This work was supported by the Priority Academic Development Program of Higher Education Institutions in Jiangsu (012062003010), the Top Talented Personnel in Six Profession in Jiangsu Province project (2010-WS-049), and the Jiangsu Province Hospital of Traditional Chinese Medicine project (2010-Y1008).

## Disclosure

The authors report no conflicts of interest in this work.

## References

- Liu A, Chen H, Wei W, et al. Antiproliferative and antimetastatic effects of emodin on human pancreatic cancer. *Oncol Rep.* 2011;26:81–89.
- Maimon Y, Karaush V, Yaal-Hahoshen N, et al. Effect of Chinese herbal therapy on breast cancer adenocarcinoma cell lines. *J Int Med Res.* 2010;38:2033–2039.
- Li Q, Cheng H, Zhu G, et al. Gambogic acid inhibits proliferation of A549 cells through apoptosis-inducing and cell cycle arresting. *Biol Pharm Bull.* 2010;33:415–420.
- Mu R, Lu N, Wang J, et al. An oxidative analogue of gambogic acid-induced apoptosis of human hepatocellular carcinoma cell line HepG2 is involved in its anticancer activity in vitro. *Eur J Cancer Prev.* 2010;19:61–67.
- Gu H, Rao S, Zhao J, et al. Gambogic acid reduced Bcl-2 expression via p53 in human breast MCF-7 cancer cells. *J Cancer Res Clin Oncol.* 2009;135:1777–1782.
- Yi T, Yi Z, Cho SG, et al. Gambogic acid inhibits angiogenesis and prostate tumor growth by suppressing vascular endothelial growth factor receptor 2 signaling. *Cancer Res.* 2008;68:1843–1850.

7. Wang TT, Wei J, Qian XP, Ding YT, Yu LX, Liu BR. Gambogic acid, a potent inhibitor of survivin, reverses docetaxel resistance in gastric cancer cells. *Cancer Lett.* 2008;262:214–222.
8. Lu N, Yang Y, You QD, et al. Gambogic acid inhibits angiogenesis through suppressing vascular endothelial growth factor-induced tyrosine phosphorylation of KDR/Flk-1. *Cancer Lett.* 2007;258:80–89.
9. Li R, Chen Y, Zeng LL, et al. Gambogic acid induces G0/G1 arrest and apoptosis involving inhibition of SRC-3 and inactivation of Akt pathway in K562 leukemia cells. *Toxicology.* 2009;262:98–105.
10. Cheng FY, Su CH, Yang YS, et al. Characterization of aqueous dispersions of Fe<sub>3</sub>O<sub>4</sub> nanoparticles and their biomedical applications. *Biomaterials.* 2005;26:729–738.
11. Peer D, Karp JM, Hong S, Farokhzad OC, Margalit R, Langer R. Nanocarriers as an emerging platform for cancer therapy. *Nat Nanotechnol.* 2007;2:751–760.
12. Martin W. Natural and synthetic polymers as inhibitors of drug efflux pumps. *Pharm Res.* 2008;25:500–511.
13. Chen BA, Lai BB, Cheng J, et al. Daunorubicin-loaded magnetic nanoparticles of Fe<sub>3</sub>O<sub>4</sub> overcome multidrug resistance and induce apoptosis of K562-n/VCR cells *in vivo*. *Int J Nanomedicine.* 2009;4:201–208.
14. Sun Q, Chen BA, Wang XM, et al. Preparation of Fe<sub>3</sub>O<sub>4</sub>-magnetic nanoparticles loaded with adriamycin and its reversal of multidrug resistance *in vitro*. *Zhongguo Shi Yan Xue Ye Xue Za Zhi.* 2007;15:748–751. Chinese.
15. Wang X, Zhang R, Wu C, et al. The application of Fe<sub>3</sub>O<sub>4</sub> nanoparticle in cancer research: a new strategy to inhibit drug resistance. *J Biomed Mater Res A.* 2007;80A:852–860.
16. Chen BA, Liang YQ, Wu WW, et al. Synergistic effect of magnetic nanoparticles of Fe<sub>3</sub>O<sub>4</sub> with gambogic acid on apoptosis of K562 leukemia cells. *Int J Nanomedicine.* 2009;4:251–259.
17. Schatz JH. Targeting the PI3K/AKT/mTOR pathway in non-Hodgkin's lymphoma: results, biology, and development strategies. *Curr Oncol Rep.* 2011;13:398–406.
18. Brazil DP, Hemmings BA. Ten years of protein kinase B signalling: a hard Akt to follow. *Trends Biochem Sci.* 2001;26:657–664.
19. Rychahou PG, Jackson LN, Silva SR, Rajaraman S, Evers BM. Targeted molecular therapy of the PI3K pathway: therapeutic significance of PI3K subunit targeting in colorectal carcinoma. *Ann Surg.* 2006;243:833–842.
20. Khaleghpour K, Li Y, Banville D, et al. Involvement of the PI3-kinase signaling pathway in progression of colon adenocarcinoma. *Carcinogenesis.* 2004;25:241–248.
21. Johnson SM, Gulhati P, Rampy BA, et al. Novel expression patterns of PI3K/Akt/mTOR signaling pathway components in colorectal cancer. *J Am Coll Surg.* 2010;210:767–768.
22. Wang J, Kuropatwinski K, Hauser J, et al. Colon carcinoma cells harboring PIK3CA mutations display resistance to growth factor deprivation induced apoptosis. *Mol Cancer Ther.* 2007;6:1143–1150.
23. Liu Y, Chen L, Ko TC, Fields AP, Thompson EA. Evii is a survival factor which conveys resistance to both TGF- $\beta$  and Taxol-mediated cell death via PI3K/Akt. *Oncogene.* 2006;25:3565–3575.
24. Roulin D, Cerantola Y, Dormond-Meuwly A, Demartines N, Dormond O. Targeting mTORC2 inhibits colon cancer cell proliferation *in vitro* and tumor formation *in vivo*. *Mol Cancer.* 2010;9:57.
25. Zhao W, Zhou SF, Zhang ZP, Xu GP, Li XB, Yan JL. Gambogic acid inhibits the growth of osteosarcoma cells *in vitro* by inducing apoptosis and cell cycle arrest. *Oncol Rep.* 2011;25:1289–1295.
26. Zhang L, Yi Y, Chen J, et al. Gambogic acid inhibits Hsp90 and deregulates TNF- $\alpha$ /NF- $\kappa$ B in HeLa cells. *Biochem Biophys Res Commun.* 2010;403:282–287.
27. Fernandez-Pacheco R, Valdivia JG, Ibarra MR. Magnetic nanoparticles for local drug delivery using magnetic implants. *Methods Mol Biol.* 2009;544:559–569.
28. Darton NJ, Hallmark B, Han X, Palit S, Slater NK, Mackley MR. The in-flow capture of super-paramagnetic nanoparticles for targeting therapeutics. *Nanomedicine.* 2008;4:19–29.
29. Wu WW, Chen BA, Cheng J, et al. Biocompatibility of Fe<sub>3</sub>O<sub>4</sub>/DNR magnetic nanoparticles in the treatment of hematologic malignancies. *Int J Nanomedicine.* 2010;5:1079–1084.
30. Semba S, Itoh N, Ito M, Harada M, Yamakawa M. The *in vitro* and *in vivo* effects of 2-(4-morpholinyl)-8-phenyl-chromone (LY294002), a specific inhibitor of phosphatidylinositol 3'-kinase, in human colon cancer cells. *Clin Cancer Res.* 2002;8:1957–1963.
31. Yamaguchi K, Lee SH, Eling TE, Baek SJ. Identification of nonsteroidal anti-inflammatory drug-activated gene (NAG-1) as a novel downstream target of phosphatidylinositol 3-kinase/AKT/GSK-3 $\beta$  pathway. *J Biol Chem.* 2004;279:49617–49623.
32. Datta SR, Brunet A, Greenberg ME. Cellular survival: a play in three Acts. *Genes Dev.* 1999;13:2905–2927.
33. Gao N, Flynn DC, Zhang Z, et al. G1 cell cycle progression and the expression of G1 cyclins are regulated by PI3K/AKT/mTOR/p70S6K1 signaling in human ovarian cancer cells. *Am J Physiol Cell Physiol.* 2004;287:C281–C291.
34. Liu P, Cheng H, Roberts TM, Zhao JJ. Targeting the phosphoinositide 3-kinase pathway in cancer. *Nat Rev Drug Discov.* 2009;8:627–644.
35. Datta SR, Dudek H, Tao X, et al. Greenberg Akt phosphorylation of BAD couples survival signals to the cell-intrinsic death machinery. *Cell.* 1997;91:231–241.
36. Zha J, Harada H, Yang E, Jockel J, Korsmeyer SJ. Serine phosphorylation of death agonist BAD in response to survival factor results in binding to 14-3-3 not BCL-XL. *Cell.* 1996;87:619–628.
37. Kim MR, Jeong EG, Chae B, et al. Pro-apoptotic PUMA and anti-apoptotic phospho-BAD are highly expressed in colorectal carcinomas. *Dig Dis Sci.* 2007;52:2751–2756.
38. Yip WK, Leong VC, Abdullah MA, Yusoff S, Seow HF. Overexpression of phospho-Akt correlates with phosphorylation of EGF receptor, FKHR and BAD in nasopharyngeal carcinoma. *Oncol Rep.* 2008;19:319–328.
39. Zimmermann KC, Bonzon C, Green DR. The machinery of programmed cell death. *Pharmacol Ther.* 2001;92:57–70.

## International Journal of Nanomedicine

### Publish your work in this journal

The International Journal of Nanomedicine is an international, peer-reviewed journal focusing on the application of nanotechnology in diagnostics, therapeutics, and drug delivery systems throughout the biomedical field. This journal is indexed on PubMed Central, MedLine, CAS, SciSearch®, Current Contents®/Clinical Medicine,

Submit your manuscript here: <http://www.dovepress.com/international-journal-of-nanomedicine-journal>

Dovepress

Journal Citation Reports/Science Edition, EMBASE, Scopus and the Elsevier Bibliographic databases. The manuscript management system is completely online and includes a very quick and fair peer-review system, which is all easy to use. Visit <http://www.dovepress.com/testimonials.php> to read real quotes from published authors.